Dihydroorotate dehydrogenase from the phytopathogenic Oomycete *Phytophthora infestans* as a novel target for crop control.

M. F. Garavito (†‡), L. García (‡†), G. Lozano(†), A. Bernal (‡), S. Restrepo (‡*), B. H. Zimmermann (†*)

(†) Grupo de investigaciones en Bioquímica y Biología Molecular de Parásitos BBMP, (‡) Laboratorio de Micología y Fitopatología Universidad de los andes LAMFU, Universidad de los Andes, Bogotá D.C., Colombia

* Corresponding authors. E-mails: srestrep@unaindes.edu.co and bazimmer@uniandes.edu.co

* Both authors contributed equally to the work

Abstract

The oomycete *Phytophthora infestans* (Mont.) de Bary, the causal agent of the tomato and potato late blight, causes tremendous crop and economic losses worldwide. In Colombia this pathogen is currently a devastating risk for the highlands dedicated to production of potato and tomato, hosts of this oomycete. Yet, current control strategies are far from being adequate and new ones are urgently needed. An interesting and unexplored alternative to control human parasites based on the inhibition of the *de novo* pyrimidine biosynthetic pathway might work as well in *P. infestans.* In this study we investigated the pathogen's dihydroorotase dehydrogenase DHODase, which catalyzes the fourth and only redox step of the pathway as a target to develop control strategies. We propose that this enzyme is member of the DHODase family 2, which compromises a mitochondrial bound enzyme with quinones as direct electron acceptors. *In silico*, preliminary molecular docking assays using homology modeled structures reveal that key structural aspects of the enzyme such as its apparent binding site flexibility could be exploited to develop species-selective inhibitors. A full length and an N-terminally truncated DHODase were expressed as recombinant proteins and complemented a DHODase-deficient bacterial host.

Keywords: Dihydroorotase dehydrogenase; inhibitor binding; pyrimidine biosynthesis; *Phytophthora infestans*; molecular docking; complementation.

1. Introduction

Within the class Oomycota are the species of the genus *Phytopthora* which are all considered serious plant pathogens and are annually responsible for huge economic losses in agriculture (Lamour *et al*., 2007; Attard *et al*., 2008). *Phytophthora infestans,* the causal agent of the potato and tomato late blight stands out in this group because of its historical importance, present incidence, aggressiveness and difficult control (Judelson HS., 2007; Fry W., 2008). Since the Irish potato famine in the 19th century this pathogen has been thoroughly studied, nevertheless, totally effective control strategies are currently not available (Nicholls H., 2004). In general oomycets like *P. infestans* have fungus-like growth morphology but share little taxonomic affinity with true fungi, lacking most of the targets attacked by fungicides used for crop management (Attard *et al*., 2008). Effective chemical fungicides such as Mefenoxam also work in *P. infestans,* however, the appearance of resistant among isolates is increasingly frequent (Son *et al*., 2004; Attard *et al*., 2008). Other effective fungicides, in order to work properly must be applied several times in massive quantities during the same production cycle, causing severe environmental effects and subsequent economic losses for farmers (Fry W., 2008). Therefore a great effort is required to develop new approaches that could lead to the discovery of more effective control strategies. As Oomyces seem to be more closely related to the apicomplexan parasites than to true fungi (Lamour *et al*., 2007; Martens *et al*., 2008) and since striking similarities between their mechanisms of pathogenicty have been recently discovered (Haldar *et al*., 2006), it is quite reasonable to believe that inhibiting similar metabolic processes shared between pathogens as diverse as oomycets and apicomplexa could be work even better that those shared

between fungi and oomycetes. This renders a new approach that could be exploited in the design of novel drugable targets with the potential to control efficiently these difficult pathogens (Haldar et al., 2006).

One of the most promising targets that has been proposed for the control apicomplexan parasites are the enzymes of *de novo* pyrimidine biosynthesis (Hyde JE., 2007). The relevance of this pathway lies in the pyrimidines which are essential and necessary for all fundamental process in organism. Pyrimidines play a central role in cellular metabolism as constituents of DNA and RNA, energy source as well as precursors of primary and secondary metabolites among others (Schroder *et al*., 2005; Evans *et al*., 2004; Löffler *et al*., 2005). In general pyrimidines can be obtained by a *de novo* biosynthetic pathway using low molecular weight precursors or by recycling via the salvage pathway and specialized transporters of endogenous or exogenous nucleosides and bases (Schroder *et al*., 2005; Evans *et al*., 2004). Under normal circumstances multicellular organisms can supply their pyrimidine requirements by the salvage pathway (Löffler *et al*., 2005). However, rapidly dividing cells in growing tissues, cancer cells, and pathogens such as fungi or parasites seem to require higher concentrations of pyrimidines, which generate a greater dependence on *de novo* synthesis (Zameitat *et al*., 2006). In apicomplexan parasites, the inhibition of *de novo* pathway has a profoundly negative effect on the virulence, growth and replication of the pathogen (Fox *et al*., 2002). Pyrimidine metabolism has not received much attention in any Omycete and has been only addressed indirectly. Still, in *P infestans* germination it seems that pyrimidines are obtained to a greater extent from the *de novo* pathway than from salvage (Clark *et al*., 1978). A different scenario is observed for its *solanum* hosts, where different tissues of the plant require a differential proportion from each pathway (Geigenberger *et al*., 2005; Schroder *et al*., 2005).

Any of the six enzymatic activities of the *de novo* pyrimidine biosynthetic pathway could be considered as a potential inhibitory target (Christopherson *et al*., 2002). However, the fourth enzymatic reaction catalyzed by dihydroorotate dehydrogenase DHODase displays a particularly stronger potential (Baldwin *et al*., 2005). Firstly due to experimental work in humans, where the DHODase is a validated target for drug developmet to treat cancer, rheumatoid arthritis and certain autoimmune diseases (Rückemann *et al*., 1998; Koyarik *et al*., 2003), which demonstrate that inhibitory drugs can effectively block the target pathway *in vivo* (Herrmann *et al*., 2000). Secondly, as x-ray crystal structures of many eukaryotes DHODases bound to different inhibitors have been solved (Walse *et al*., 2008; Majbritt *et al*., 2004; Deng *et al*., 2009), they provide clear evidence that species-selective inhibitors can be developed. These two lines of evidence suggest that selective inhibitors could be developed for *P. infestans,* that could exert low or none effect on the host enzyme and could be amenable in a crop control strategy.

DHODases have been classified in two families based on their cytoplasmic or membrane-bound cellular locations (Björnberg *et al*., 1997), as well as their capacity to utilize different electron acceptors to reoxidize FMNH2. While cytoplasmic enzymes (Family1) utilize fumarate and NAD+ as electron acceptors, membrane-bound enzymes (Family 2) require respiratory quinones (Hansen *et al*., 2004). Additionally, family 2 enzymes display variable length N-terminal extensions which are longer than those in family 1 and are associated with their location (Rawls *et al*., 2000). The general mechanism of action of family 1 and 2 DHODases is to catalyze the oxidation of dihydroorotae to orotate with a reduction of the flavin cofactor FMN. The second part of the reaction varies depending on the family; for eukaryotes with mitochondrial bound family 2 DHODases, FMNH2 transfers these electrons to respiratory chain quinones (Jones ME., 1980; Rawls *et al*., 2000). The connection between the DHODase and the mitochondrial respiration has made many potential inhibitory compounds fail clinical approval, as they could also interfere with the respiratory chain activities (Knecht *et al*., 2000).

High throughput screening is still one of the most common techniques to find new lead compounds with inhibitory effects on DHODases (Baldwin *et al*., 2005). Nevertheless, the expensive and time-consuming experimental screening of compound libraries also involves posterior work to further optimize the results obtained (Deng *et al*., 2009).

Currently, the evolution of rapid techniques for virtual screening of compound libraries has become an integral part in the drug discovery process providing rational and low cost alternatives in the search for lead compounds (Rarey *et al*., 1995). In particular protein ligand docking software has allowed testing, finding and modifying *in silico* inhibitory compounds of DHODases (Ananthula *et al*., 2008; Pospisil *et al*., 2002).
In the case of *P. infestans*, the interest in studying this pathway goes further than just describing this metabolism in Oomycets for a better understanding and relies on its in, its potential for developing novel strategies for crop control. In the present study we have used a mixed strategy (computer assisted/experimental) based on the DHODase of *P. infestans* to evaluate if the enzymes of *de novo* pyrimidine biosynthesis can be used as targets for the development of highly specific Oomycidal inhibitors.

2. Material and methods

2.1 Strains and growth Condition

P. infestans strain 1043 (A1 mating type, mitochondrial DNA IIa) and 4084 (A2 mating type, mitochondrial DNA Ia) were used throughout this study; isolates were obtained in Colombia from a *Solanum tuberosum* and a *Physalis peruviana* host, respectively (Vargas *et al.,* 2009). The isolates were cultured routinely on rye agar medium and incubated at 17ºC for eight days in the dark (Goodwin *et al*., 1998). Mycelia for genomic DNA extractions were obtained by growing the strain in the dark on Pea-broth medium for 15-20 days at 18ºC (Goodwin *et al*., 1992). The developmental stages (mycelia, sporangia, zoospores and cysts) for isolation of RNA were obtained according to van West *et al*. (1998).

2.2 PCR amplification, cloning and sequencing

Genomic DNA from mycelia was used as template for PCR amplification of the *P. infestans* DHODase gene, since the putative genomic sequence of dihydroorotate dehydrogenase mitochondrial precursor in locus PITG_01913 lacks introns http://www.broadinstitute.org. For expression purposes, 2 vectors were constructed to express a full length and an N-terminally truncated version of the gene. The following synthetic oligonucleotides were designed to amplify the gene. The primers for the full length protein PiDHODs 5'-CA**GGATCC**TATGCGAGCAGCGACGTTCTC-3', PiDHODas 5'-CAGGATCCTTACTTGTGAGCAGCGCCTACG 3', which generate a 1275bp DNA, fragment. For the N-terminally amplify truncated version, primer PiDHODas remains the same while the PiDHODs was replaced with PiDHODs2, 5'-CA**GGATCC**TCCGCATGAGTGGGTCATC-3', which generate a 1113bp DNA fragment, (BamHI restriction sites shown in boldface). Fresh PCR products were adenylated and ligated in the pGMT-Easy vector (Promega) according to the manufacturer's instructions, prior to their cloning in *E. coli* DH5-α electro-competent cells (Stratagene). The cloned pGMT-Easy-PiDHOD and pGMT-Easy-ΔNPiDHOD gene fragments were confirmed by sequencing (Macrogen, Korea), using PCR products obtained with M13 primers following the amplification and purification of plasmid DNA. These verified recombinant plasmids either containing the full length or the truncated version of the DHODase gene were digested with BamHI restriction enzyme (Promega) and separated by 1% agarose gel electrophoresis. The PCR products were extracted using a gel purification kit (BIO-101) and ligated into the pET-19b expression vector (Novagen) which had been similarly treated after removal of the phosphates from the ends with calf intestine alkaline phosphatase (Invitrogen). The constructs where transformed into *E. coli* BL21CodonPlus(DE3) electro-competent cells with a Micropulser Electroporator (BioRad,). The recombinant proteins expressed from this vector are referred to as PiDHOD and ΔNPiDHOD-PHEW, and both have a 10 N-terminal His residues fusion tag.

2.3 Expression and purification

Transformed *E. coli* BL21 electro competent cells were precultured in Luria-Bretani broth medium (LB) with 100µg/ml ampicillin as selection marker and allowed to grow overnight at 37°C at 200rpm agitation. The preculture was diluted to 5% in LB

containing 100µg/ml ampicillin and grown at 37°C till OD_{620nm}=0.5-0.6. The overexpression of the full length ~48.54 kD and the N-terminus truncated ~43.18 kD enzymes was induced with 1mM Isopropil β–D-thiogalactopyranoside (IPTG), supplemented with 0.1mM flavin mononucleotide (FMN) and growth was continued overnight at 25°C (Baldwin et al, 2002). The induced culture was harvested by centrifugation at 3500g for 15 minutes at 4°C, supernatant discarded and cell paste frozen at -80°C until use. Typically, 1,2 g of cell paste was obtained per 250ml of liquid culture. Frozen cell paste (of ≈ 86 ml culture) was suspended in 5ml of lysis buffer (50mM Tris pH8.5, 2mM 2-mercaptoethanol, 2% triton X-100, 0.5mM FMN, 10% glycerol and 1 mg /ml lysozyme) and incubated for overnight on ice in the presence of a protease inhibitor cocktail (200mM phenylmethylsulfonyl fluoride, 10ug/ml benzamidine, 1ug/ml leupeptine, 2ug/ml antipain and 1ug/ml chymostatin) (Baldwin *et al*, 2002). The cell suspension was disrupted by sonication for 25 x 20 second bursts with amplitude of 3, on ice (Heat systems Ultrasonic). The lysate was centrifuged at 8,500 g for 1 hour at 4°C.

For purification of recombinant protein 5ml columns were loaded with 2ml of Ni-NTA resin (Qiagen) equilibrated with buffer A (50mM Tris/HCl pH8.5, 300mM NaCl, 2mM 2-mercaptoethanol, 20mM imidazol, 0,5% Triton X-100, 0.1mM FMN and 10% gycerol). The centrifuged soluble fraction (≈ 4,5ml) was loaded on the column, washed with 10 volumes of buffer A and with 10 volumes of buffer B (50mM Tris/HCl pH8.5, 300mM NaCl, 2mM 2-mercaptoethanol, 40mM imidazol, 0,5% Triton X-100, 0.1mM FMN and 10% glycerol). The recombinant protein was eluted with a step gradient of imidazole from 20mM to 500mM in buffer C (50mM Tris/HCl pH8.5, 300mM NaCl, 2mM 2-mercaptoethanol, 0,5% Triton X-100, 0.1mM FMN, 10% glycerol plus Imidazol) (Baldwin et al, 2002). The recombinant DHODase was eluded from the column in the fraction with 300mM of Imidazole in buffer C, its purity checked on 12% SDS-PAGE gel electrophoresis, and stored at -80°C till needed. Protein concentration during purification was determined by means of the bicinchoninic acid protein assay with bovine serum albumin as standard using the BCA protein assay (Pierce) according to manufacture's specifications. For enzymatic activity assays fractions where subjected to buffer exchange performed with PD-10 columns (Sephadex G-25-M,GE Healthcare) with buffer D (50mM Tris/HCl pH8.5, 150mM NaCl, 0,1% Triton X-100 and 10% glycerol) (Ullrich et al., 2001).

2.4 Complementation Assay

Cloned sequences for the full length pGMT-Easy-PiDHOD and the N-terminus truncated pGMT-Easy-ΔNPiDHOD were analyzed by means of complementing DHODase-deficient *E. coli* cells (ATCC12632, *pyrD* (-)). This strain is unable to grow in minimal media unless supplemented with uracil (Sierra Pagan *et al*., 2003). Verified recombinant plasmids either containing the full-length or the truncated version of the DHODase gene were digested with BamHI restriction enzyme (Promega) and separated by 1% agarose gel electrophoresis. Appropriate products were extracted using a gel purification kit (BIO-101) and ligated into a Topo-TA (Invitrogen) plasmid which had been removed with BamHI and calf intestinal phosphatase (Invitrogen). After transformation of the *E. coli* DHODase-deficient electro-competent cells with the ligation mixture, colonies were selected by grow in 100ug/ml ampicillin on agar plates of minimal media (MM), (glucose 5g/l, Na_2HPO_4 6g/l, KH_2PO_4 3g/l, NH_4Cl 1g/l, NaCl 0,5g/l, $MgSO_4$ 0,12g/l, $CaCl_2$ 0,01g/l). Plasmid DNA was isolated from several independent colonies of TOPO-PiDHOD and TOPO-ΔNPiDHOD and verified by PCR with the respective primers. Transformed *pyrD* (-) electro competent cells *E. coli* cells were precultured overnight in LB with 100µg/ml ampicillin as selection marker plasmid transformed cells. The preculture was diluted to 1% in MM containing 100µg/ml ampicillin for parent, full length and truncated plasmids and without ampicillin for *pyrD* (-) cells. 12ug/ml of uracil were added to a copy of parent vector and for *pyrD* (-) cells. OD at 600nm was recorded every hour until log phase was reached.

2.5 SDS-PAGE and electrotransfer

Protein samples were fractionated by SDS-PAGE on 12% running gels, with 5% stacking gels, using the buffer system described by Laemmli (1970). Electrophoresis

was performed in a BioRad Mini-Protean II electrophoresis cell for 1 hour, at 200 volts, constant voltage. Gels were visualized by staining with Coomassie Blue G-250 dye. Protein samples were electrotransferred from gels to 0,45 µm nitrocellulose membranes (Sigma) using a BioRad Mini Trans-Blot, for 1 hour at 100 volts. Membranes were incubated for an hour with 5% nonfat dry milk, washed and incubated for 2 hours with anti-Histag antibodies 0.1ng/ml (Qiagen). Membranes were washed, followed by anti-rabbit horse radish peroxidase conjugate (Sigma), at dilutions of 1:1500. Bound antibodies were visualized by adding 4-chloro-1-napthol at 0.3% in methanol (Zimmermann *et al*., 1993) and 30% H_2O_2 (bands started to appear at the 3rd minute).

2.6 DHODase Phylogenies

A homology search of the putative DHODase gene sequence was performed using in the *P. infestans* genome project (http://www.broadinstitute.org). Pair-wise and multiple sequence alignment of the PiDHODase with representative organisms from other taxa (Nara *et al*., 2000) were performed using the Muscle program (Edgar R.C, 2004). These alignments were manually edited in JalView, leaving out poorly-aligned regions. Phylogenetics analysis using the amino acid sequences of different DHODases were performed by maximum likelihood (ML) using the PhyML program (Guindon et al., 2003). The model of amino acid substitution used was LG+I+G selected with the ProtTest program (Abascal et al., 2005). A consensus tree was generated with a boostrap analysis and the parameters were MV 13603, G 1,603 and I 0,032. The support of the branches is calculated from a 1000 resampling bootstrap. The sequences used in this study were collected from GenBank database or genome projects. The sequences data collected from databases are as follows, with accession number in parenthesis: *Synechococcus elongates (*BAD79412), *Neisseria gonorrhoeae* (AAW90382), *Escherichia coli* (P0A7E1), *Salmonella typhimurium* (NP_460032), *Agrocybe aegerita* (AAA32636), *Caulobacter crescentus* (ACL94027), *Thalassiosira pseudonana* (EED92525), *Phaeodactylum tricornutum* (EEC45222), *Aspergillus nidulans* (CBF70590), *Schizosaccharomyces pombe* (CAB08175), *Homo sapiens* (BAF84982), *Mus musculus* (AAH45206), *Rattus norvegicus* (CAA56765), *Vitis vinifera* (CAO70164), *Nicotiana tabacum* (CAC35420.1), *Solanum tuberosum* (SGN-U272884), *Arabidopsis thaliana* (CAA44695), *Zea mays* (ACG45575), *Drosophila melanogaster* (NP_599138), *Drosophila melanogaster* (NP_477224), *Plasmodium falciparum* (BAB85127), *Toxoplasma gondii* (AAM46067), *Caenorhabditis elegans* (AAK21481), *Phytophthora ramorum* (Phyra1_1|72251), *Phytophthora sojae* (Physo1_1|109029), *Phytophthora infestans* (PITG_01913.1), *Phytophthora capsici* (PhycaF7|45501), *Saccharomyces cerevisiae* (CAA53557), *Lactococcus lactis* (AAK05650), *Trypanosoma cruzi* (3C3N_D), *Leishmania amazonensis* (BAA94299), *Lactobacillus plantarum* (CAJ75873), *Bacillus caldoyticus* (CAA51741), *Bacillus subtilis* (CAB13418), *Enterococcus faecalis* (AAP04498), *Lactococcus lactis* (AAK05444), *Sulfolobus acidocaldarius* (CAD31980), *Aquifex aeolicus* (AAC06426) and *Pyrococcus furiosus* (AAL81663).

2.7 DHODase models

The protocol used to derive the DHODases structural models from *P.infestans, S tuberosum* and *Candida albicans* consisted in four phases: target selection, sequence alignment, model building, and model evaluation. The primary sequence of PiDHODase, StDHODase and CaDHODase were taken from the genome projects and the GenBank. Homology models were built with the SWISS-MODEL server (Schwede *et al*., 2003) using the Automatic Modelling Mode which selected as modeling template for all DHODases, the crystal structures of *Homo sapiens* (2B0M) with a 2.0 Å resolution (Hurt et al., 2006) from the RCSB Protein Data Bank**.** A sequence alignment of DHODases annotated with information from the DHODase crystal structures of *P. falciparum, Rattus rattus, H. sapiens, E. coli ,* or the predicted structures of *P. infestans, S. tuberosum* and *C. albicans* was constructed using the multiple sequence alignment program Clustal W (Thompson *et al*., 1994) and is presented in Figure 1. The final homology models generated by Swiss-model were inspected and checked with the SwissPdb-Viewer (Kaplan *et al*., 2001; Guex *et al*., 1997), so that 90% of the amino acids residues fall within the acceptable region of the Ramachandran plot. For docking purposes all models were overlaid by superimposing the key residues over the *P. falciparum* structure (PDB code 1TV5) in the SwissPdb-Viewer. The models were

further prepared for docking in Molegro virtual docker software, where they were automatically assigned charges and protonation states (Thomsen *et al*., 2006).

2.8 Ligand selection

Since specific inhibitors for the PiDHODase have not yet been described, we tried to determine *in silico* the inhibitory plausibility of some commercial compound using the generated models and the crystallographic structures of DHODases. For these purposes 20 known compounds that exert an inhibitory activity against human, rat or malarial DHODases and that were bound to their crystal structures were selected. In essence, these twenty could be grouped into 4 types based in their structural similarity to brequinar, atovaquone, leflunomide and triazolopyrimidine. Nine compounds bound to crystal structures of other enzymes were selected as well to join the docking list, as they were implicated in interfering with the electron transport in mitochondria or pyrimidine metabolism. Various natural and artificial acceptors of DHODases bound to crystallographic structures of other enzymes (15 in total) were selected in order to get a picture of the binding mode of the acceptor. The compound data collected from the RCSB Protein Data Bank is as follows, compound name, with the PDB code of enzyme and ligand in parenthesis: 5-METHYL-7-(NAPHTHALEN-2-YLAMINO)-1H-[1, 2,4]TRIAZOLO[1,5-A]PYRIMIDINE-3,8-DIIUM (3I65, JZ8-1001), N-ANTHRACEN-2-YL-5-METHYL[1,2,4]TRIAZOLO [1,5- A]PYRIMIDIN-7-AMINE (3I68, JZ4-1001), 5-METHYL-N-[4-(TRIFLUOROMETHYL)PHENYL][1 ,2,4]TRIAZOLO[1,5- A]PYRIMIDIN-7-AMINE (6I6R, J5Z-1001), (2Z)-N-BIPHENYL-4-YL-2-CYANO-3-HYDROXYBU T- 2-ENAMIDE (3F1Q, BCE-397), (2Z)-2-CYANO-N-(2,2'-DICHLOROBIPHENYL-4- YL)- 3-HYDROXYBUT-2-ENAMIDE (3FJ6 ,CIH-399), (2Z)-2-CYANO-N-(3'-ETHOXYBIPHENYL-4-YL)- 3- HYDROXYBUT-2-ENAMIDE (3FJL,CJH-399), (2Z)-N-(3-CHLORO-2'-METHOXYBIPHENYL-4-YL)- 2-CYANO-3-HYDROXYBUT-2-ENAMIDE (3G0U,MDY-2), (2Z)-N-BIPHENYL-4-YL-2-CYANO-3-CYCLOPROP YL- 3-HYDROXYPROP-2-ENAMIDE (3G0X, MD7-2), 6-CHLORO-2-(2'-FLUOROBIPHENYL-4-YL)-3-METHYLQUINOLINE-4-CARBOXYLIC ACID (2PRH, 238-400), 5-METHOXY-2-[(4-PHENOXYPHENYL)AMINO] BENZOIC ACID (2PRL, 2RC-400), 2-({[3,5-DIFLUORO-3'-(TRIFLUOROMETHOXY)B IPHENYL- 4-YL]AMINO} CARBONYL) CYCLOPENT-1-ENE-1-CA RBOXYLIC ACID (2FPT, ILB-405), 3-{[(3-FLUORO-3'-METHOXYBIPHENYL-4-YL)AM INO]CARBONYL}THIOPHENE- 2-CARBOXYLIC ACID (2FPV, ILC-405), 3-({[3,5-DIFLUORO-3'-(TRIFLUOROMETHOXY)B IPHENYL- 4-YL]AMINO}CARBONYL)THIOPHENE-2-CARBOXYL IC ACID (2FPY, ILF-407), 2-({[2,3,5,6-TETRAFLUORO-3'-(TRIFLUOROME THOXY)BIPHENYL- 4-YL]AMINO}CARBONYL)CYCLOPENTA-1,3-DIENE - 1-CARBOXYLIC ACID (2FQI, ILH-600), 2-({[3-FLUORO-3'-(TRIFLUOROMETHOXY)BIPHE NYL- 4-YL]AMINO}CARBONYL)CYCLOPENT-1-ENE-1-CA RBOXYLIC ACID (2BXV,3FT-1401), 3-AMIDO-5-BIPHENYL-BENZOIC ACID (2B0M,201-401), 2-CYANO-3-HYDROXY-N-(4-TRIFLUOROMETHYL-P HENYL)- BUTYRAMIDE (1TV5, A26-1001), 2-[4-(4-CHLOROPHENYL)CYCLOHEXYLIDENE]-3, 4- DIHYDROXY-1(2H)-NAPHTHALENONE (1UUM, AFI-400), 6-FLUORO-2-(2'-FLUORO-1,1'-BIPHENYL-4-YL)- 3-METHYLQUINOLINE-4-CARBOXYLIC ACID (1UUO, BRF-1397), 2-BIPHENYL-4-YL-6-FLUORO-3-METHYL-QUINOL INE- 4-CARBOXYLIC ACID (1D3G, BRE-397), 3,4-DIHYDROXYBENZOIC ACID (3DX5, DHB-289), 5-FLUOROURACIL (1H7X, URF-1033), 2-(ACETYLOXY)BENZOIC ACID (3IAZ,AIN-1202), 2-METHYL-N-PHENYL-5,6-DIHYDRO-1,4-OXATHI INE- 3-CARBOXAMIDE (2WDQ, CBE-1130), CLINDAMYCIN (1YJN, CLY-9000), MENADIONE (1TUV,VK3-4548), SALICYLHYDROXAMIC ACID(3GCJ, SHA-617), 2-HYDROXYBENZOIC ACID (3GF2, SAL-147), UBIQUINONE-10 (1OGV, U10-1305), UBIQUINONE-8 (3E8T, UQ8-221), UBIQUINONE-1(2ZUQ, UQ1-177), UBIQUINONE-2(2UWU, UQ2-1287), 2,3-DIMETHOXY-5-METHYL-6-(3,11,15,19-TET RAMETHYL- EICOSA-2,6,10,14,18-PENTAENYL)-[1,4]BENZOQUINONE (2GMH, UQ5-612), 5-(3,7,11,15,19,23-HEXAMETHYL-TETRACOSA- 2,6,10,14,18,22- HEXAENYL)-2,3-DIMETHOXY-6-METHYL-BENZENE - 1,4-DIOL(2IBZ, UQ6-506), UBIQUINONE-7 (1VRN, UQ7-502), 2-DECYL-5,6-DIMETHOXY-3-METHYLCYCLOHEXA- 2,5- DIENE-1,4-DIONE(3HYW, DCQ-500), 1,4-BENZOQUINONE(3B6K, PLQ-201), 2,3-DIMETHYL-5-(3,7,11,15,19,23,27,31,35 - NONAMETHYL-2,6,10,14,18,22,26,30,34-HEXA TRIACONTANONAENYL- 2,5-CYCLOHEXADIENE-1,4-DIONE-2,3-DIMETHY L- 5-SOLANESYL-1,4-BENZOQUINONE(3BZ1, PL9-367), FUMARATE(2EE0, FMR-501), UNDECYL-MALTOSIDE (2E74; UMQ-1101), PHYLLOQUINONE (2O01; PQN-501), 2,3-DIMETHYL-1,4-NAPHTHOQUINONE(2BS4, DMW-1244) AND N-(BIPHENYL-4-YLSULFONYL)-D-LEUCINE (3EHX, BDL-0).

2.9 Docking calculations

A structurally-based partially flexible docking software was used throughout the study, where the protein structure remains rigid while the ligand compound may adopt many orientations (positions) within the interaction site. For the crystal structures of the DHODases the solvent molecules were removed; structures, models and compounds were combined in a single macromodel. Flexible torsion of ligands was detected, when necessary hybridization and bond orders were added to ligands as well as enzymes. For

the molecular docking of the compounds to the binding site of the DHODases models or structures, we used the Molegro virtual docker. This new heuristic evolution program uses the search algorithm MolDock which has gained the attention of many investigators in the field (Sivaprakasam et al., 2009, Khan et al., 2009, Cassidy et al., 2009). An automatic procedure was used to generate a prediction of the potential binding cavities over all DHODases structures. Over all the cavities predicted, the *P. falciparum* DHODase cavity 2 displayed only the presence of the inhibitor and was the smallest. Therefore, we manually selected the size of this cavity as a grid constraint over all DHODase structures and models (X=38,38, Y=34,33 and Z=37,14). Default settings were used for docking in Molegro, with the exception of a modified binding interaction site radius of 10Å. The 5 best docking conformations or positions of each compound were evaluated in terms of MolDock, rerank and H-bond scoring functions from the MolDock [GRID] option. The best compound position was chosen on basis of a visual inspection and comparison with available experimental data. Docking took on average 5 minutes per compound in each DHODase in a Intel(R) Core (TM)2 Duo Windows XP computer with 2GB of RAM.

3. Results and discussion

3.1 *P. infestans* genes of the pathways

As pyrimidine pathways involve the synthesis, interconversion, salvage and breakdown of pyrimidine nucleotides we tried to decipher how these occur in *P. infestans*. The similarity searches over the *P. infestans* genome reveal the existence of open reading frames (ORFs) homologous to the nucleotide sequences of genes encoding for the enzymes of *de novo* pyrimidine biosynthetic pathway. They were annotated as the putative genes of the carbamoyl phosphate synthase CPSaseII, aspartate transcarbamoylase ATCase, dihydroorotase DHOase, dihydroorotate dehydrogenase DHODase, orotate phosphoribosyl transferase OPRTase and orotidine 5′-monophosphate decarboxylase OMPDase (Table 1); having the corresponding EST support. Due to the availability of other genome projects, this same identification was possible for three other *Phythopthora* species (*P. ramorum*, *P. sojae* and *P. capsici*; http://genome.jgi-psf.org) as well as for two *Solanaceous* hosts (*S. tuberosum* and *N. tabacum*; http://solgenomics.net/) (data not shown). The presence of the six genes *Phytophthora* pathogens as well as their *Solanum* hosts indicates that both are capable of biosynthesis, and correlates with the fact that this pathway is evolutionary conserved among almost all organisms; even though differences appear at the gene organization level (Nara *et al*., 2000).

In *P. infestans,* the genes of the pathway seem to be quite varied compared to other taxonomic groups (Nara *et al*., 2000), as can be seen from the annotation of the genes (Table 1), where it appears that CPSaseII as well as OPRTase and OMPDase might be duplicated. These last two genes appear to code for an inversely fused domain bifunctional protein as in parasitic trypanosomatid protists, where lateral gene transfer and synteny process occurred (Makiuchi *et al*., 2007). The presence of this synteny has gather scientific attention in *P. infestans,* as its inversion order shows a clear example of an independent fusion event (Morris *et al*., 2009). Interestingly, at the protein level these multifunctional enzymes might have an advantage in the channeling of substrates and products at higher rates in the enzymatic reactions. Based on these results (Figure 1), it seems that the last two enzymes are the most promising targets of the pathway to develop crop control strategies. Nevertheless, we believe that even slight differences between host and pathogen enzymes catalyzing other steps of the pathway (such as in DHODase) could not be ruled out for this propose.

To gain an idea whether *P. infestans* is capable, as are its *Solanum* hosts, of salvaging pyrimidines (Katahira *et al*., 2002), we searched as well for the ORFs of four genes encoding enzymes of the salvage pathway. The similarity searches showed the presence of uridine phosphoribosyl trasferase UPRTase, uridine kinase UKase, thymidine kinase TKase and dihydrofolate reductase (DHFRase) in the *P. infestans* genome (Data not shown). These findings indicate that *P. infestans* may be capable of salvaging pyrimidines, although an *in vivo* confirmation is necessary. As *P. infestans* seem to be

capable of obtaining pyrimidines by the salvage and biosynthetic pathways: the exact extent to which each one is used must be taken into account in the development of control strategies. We suspect, however, that the pyrimidine pools obtain by the salvage pathways would not be enough to sustain rapid growth and proliferation of *P. infestans* upon host invasion. Therefore the enzymes that catalyze the biosynthetic pathway could be considered as the pacemakers for this process.

3.2 Gene architecture and sequence analysis of the *P.infestans* DHOD

The gene encoding the DHODase was identified as a single copy in the supercontig 2 (locus: PITG_01913) in the *P.infestans* genome. It has an intron-lacking open reading frame (1275 bp), which encodes a 45.28kDa protein (424 residues) with an isoelectric point of 8.74. This fully is consistent with the high pI predicted for other family 2 DHODases. The derived amino acid sequence contains highly conserved binding domains for the FMN and dihydroorotate that are characteristic of all dihydroorotate dehydrogenases (Figure 1). Within the catalytic center of the *P. infestans* DHODase, a highly conserved serine residue was present, which is characteristic of family 2 membrane-bound enzymes that depend on a functional respiratory chain (Makiuchi *et al*., 2008, Nørager ., 2002, Sørensen *et al*., 2002).

A full database comparison using BLASTp (Altschul *et al*., 1997) revealed that *P. infestans* DHODase was more similar to the type 2 family of DHODases (*H. sapiens*, 56.7%; *P. falciparum*, 33.9%; *C. albicans*, 44%; *A. thaliana*, 53.4%; *E. coli*, 42.6%) and was less similar to family 1 (*T. cruzi*, 34.1%; *S. cerevisiae*, 30.3%). The *P. infestans* sequence was further aligned to selected family 1A, 1B and 2 DHODases. It was found to be more similar to the *R. norvegicus*, which has 395 residues with a molecular mass of 42.7kDa (Ullrich *et al*., 2001). The rat DHODase belongs to type 2 family and its crystal structure has already been obtained (Hansen *et al*., 2004). From the Genome databases, putative DHODases were found in the 4 *Phytophthora* species sequenced so far. As expected, the *P. infestans* enzyme had the highest identities with the other 3 *Phytopthora* species (*P. ramorum*, 86.9%; *P. sojae*, 89.6% and *P. capsici*, 89.9%). A similar analysis was performed with 2 of the *P. infestans* hosts (*S. tuberosum*, 54.5%; *N. tabacum,* 54.2%) which displayed a lower similarity. We amplified and sequenced the PiDHODase gene from two different strains isolated from potato and cape gooseberry hosts. We found that both sequences shared 100% identity at the amino acid level; this may reflect a high protein conservation even due to the selective pressure of different hosts.

We generated a phylogenetic tree using selected DHODase sequences obtained from the databases (Figure 2), which was clearly discordant with the accepted organism phylogeny. Even though, the phylogenetic relationship among the DHODases correlates well with the family's localization and catalytic properties (Nara et al., 2000, Björnberg *et al*., 1997). It seems that the DHODase from the four *Phytophthora* species are visibly more evolutionarily related to family 2 enzymes than to those of family 1. Interestingly, *Phytophthoras* DHODases share more in common with those of plants, animals and apicomplexan parasites than with those of the true fungi, whose DHODases categorized in the same family 2 (Figure 2).

Further structural comparisons of the *P. infestans* DHODase with other family 2 enzymes (Figure 1), clearly show an N-terminal extension characteristic of this family, which is absent in family 1 and relates to the protein cellular location (Löffler et al., 2002). Experimental work with the rat DHODase N-terminal extension, show it to contain a cationic mitochondrial targeting sequence (residues 2-10) and a hydrophobic transmembrane helix anchor (residues 12-28) that holds the enzyme in the inner mitochondrial membrane (Rawls *et al*., 2000). Sequence analysis of the *P. infestans* DHODase reveal a potential hydrophobic transmembrane associated anchor between residues 30-49 (Figure 1) and a putative N-terminal mitochondrial targeting signal detected by the program TargetP.1.1 (Emanuelsson *et al*., 2000). In fact, compared to rat, the 17 residue longer N-terminal extension of *P. infestans* DHODase seems to contain a unique cleavage site at position 23 (Figure 1) detected by the program MitoprotII v1.101 (Claros *et al*., 1996). These results suggest that the *P. infestans* enzyme could be directed to the inner mitochondrial membrane, which is a

characteristic of other eukaryotic DHODases that depend on a functional respiratory chain (Jones M.E., 1980). The results also suggest that a proteolytical processing of a signal peptide (first 23 residues) of the *P. infestans* DHODase could play an important role for the correct targeting on the enzyme to the mitochondrial membrane. Further experimental analysis of *P. infestans* native enzyme will provide evidence to help clarify this issue.

3.3 PiDHODase protein structure model

In silico, the homology based predicted structure of the *P. infestans* enzyme could only be generated from Met67 to Lys424. This leaves out of the model the predicted mitochondrial targeting sequence and the hydrophobic transmembrane domain of the N-terminus extension. The same was true for the N-terminus extensions of *C. albicans* and *S. tuberosum* models (not shown). Visual inspection of all structural models show similar $(\alpha/\beta)_8$ folding to that observed in the crystal structures of rat, human, *E.coli* and malarial DHODases (Figure 1). In general all DHODase can be decomposed into a large and small domain. For *P. infestans,* the small N-terminal domain (Met67-Leu91) and the large C-terminal domain (Thr92-Lys424) are connected by an extended loop (Figure 2A) that varies in length depend the organism. The large domain can be described as an $(\alpha/\beta)_8$ barrel, that contains the redox site formed by the substrate binding pocket and the cofactor (FMN) binding site (Figure 1). Whereas the small domain consists of two alpha helices (labeled as αA and αB, Figure1), connected by a short flexible loop that forms a hydrophobic entrance to the FMN group located on top of the large domain (Figure 2A). This small domain is believed to harbor the binding site of the natural ubiquinone acceptor and is the location of binding of the current human DHODase inhibitors (Baumgartner *et al*., 2006).

The models generated for the DHODases of *P. infestans*, *C.albicans* and *S. tuberosum* were structurally evaluated using Anolea, Gromos and Verify3D (Arnold et al., 2006).

The programs reveal low quality regions (low B-factor) that were observed when the predicted *P. infestans* DHOD structure was superimposed over the human 2B0M structure used as template (Figure 2A). Specifically one of these places in all the DHODase models that was extremely important, as it was clearly located in αA which is part of the inhibitor binding site and must be corrected. For these reason further refinement of the models was done manually using the optimizer and the Ramachandran Plot tools of the SwissPdb-Viewer. All refined models agreed with the values accepted for good homology models, in which more than 90% of the Cα residues lie within the allowed regions of the plot (Singh *et al*., 2008), supporting sufficiently accurate models. Nevertheless, further refining of these models using additional evaluation approximations is desirable.

In general, it was possible to obtained good homology models for the initial docking trials. However, it should be especially noted, that the first alpha helix (αA; Figure 1) of all the structures are low local quality, and may adopt quite different conformations. The analysis of rat DHODase crystal structures bound to different inhibitors, showed that remarkable differences are noticed in this first αA-helix with respect to its orientation upon the binding of inhibitors (Hansen *et al*., 2004). A similar analysis of the human DHODase illustrates the high degree of flexibility of the αA-helix and its surrounding loop residues (Walse *et al*., 2008). This reflects the fact even the best three-dimensional models produced for the DHODases are just approximations and may only serve as leads to discover compounds that could interfere with their activity.

3.4 Docking calculations

To identify *in silico* potential lead compounds that may obstruct *P.infestans* DHODase activity without actually performing expensive and time-consuming compound library

screening, we gathered a set of 29 potential inhibitory compounds to test on *P. infestans* DHODase (see material and methods). In order to further guide and verify our interpretation of docking results, the same analysis was performed with the crystal structures of rat, human, *E.coli* and malarial DHODase. For these 4 DHODase crystal structures the docking results for each inhibitor was compared to the available experimental activity data. This simple verification allowed us to empirically determine cavity threshold values (search space) in the DHODase models. It served as well as a empirical parameter to guide the interpretation of the MolDock, Rerank and H-bond scores. This empirical guide was used as the main criteria to select between possible and not-possible inhibitors, and to choose the best positions within the top-rated list.

For all the DHODase crystal structures, it was possible to identify within the docking positions the true crystallographic inhibitor binding mode conformation, with an RMSD of at less than 2Å. This shows that by the RMSD criterion, our docking prediction could be considered valid (Stroganov *et al*., 2008; Spyrakis *et al*., 2007).

To test if the empirical thresholds criteria worked on the models, we examine them first with the *C. albicans* generated model; since experimental activity data is available for comparison (Zameitat *et al*., 2006). We found a good correlation (92%) between our docking results and the experimental data, where with the best positions selected, 12 of the 13 comparable compounds were correctly rank as inhibitors and non-inhibitors. Furthermore, our results suggest that a better inhibitory activity of the *C. albicans* DHODase could be possible using compounds structurally similar to brequinar Ilf-407, Ilb-405, Ilh-600, 201-401, 238-400, 2rc-400 or 3ft-1401(Data not shown). This seems quite reasonable, since brequinar was one of compound found to exert an inhibitory effect over the *C. albicans* DHODase (Zameitat *et al*., 2006).

For the *P. infestans* DHODase model, the docking calculations reveal that among the 29 compound analyzed in this study, 55.1 % could possibly exert an inhibitory activity against the enzyme. As the selection of compounds was based on being recognized as a DHODase inhibitor a high number of candidates were expected. In fact, all of these lead compounds (16 in total) were from initially selected group of twenty (Table 2). To further improve and diminish the list of potential compound we used a counter-selection strategy (Ananthula *et al*., 2008), in which compounds that also exert an inhibitory action over the *S. tuberosum* host enzyme were removed. This selection criterion has already been applied to develop species-selective DHODase inhibitors to control the parasite *P. falciparum* without affecting the human host enzyme (Baldwing *et al*., 2005; Phillips *et al*., 2008). With this additional criterion, only 3 of the compound (J5z-1001, Jz81001 and Afi-400) remain as candidate *P. infestans* inhibitors (Table 2). Interestingly, two of these three candidate compounds were the same as the ones found to be species-selective inhibitors of the *P. falciparum* DHODase (Phillips *et al*., 2008).

These results renders the question if pathogens' DHODases (*P. infestans* and *P. falciparum*) display a similar binding mode for these potential inhibitory compounds that could differ significantly from the one exhibit by the hosts' DHODases (*H. sapiens* and *S. tuberosum*). Careful inspection of the results by graphical representation indicates that nevertheless there is no clear evidence of a conserved residue pattern or a binding mode for these compounds. Instead, different and non conserved binding modes were displayed *in silico* by the most promising compound J5z-1001 (Figure 4). Nevertheless no clear binding modes could be discovered to guide pathogen-selective inhibitor searches. Key structural features could be hypothesized, and might be used to render spatial constraints that could guide a *P. infestans* species selective inhibitor discovery. Features such as a bigger space in the inhibitor binding site that seems to be able to receive larger compounds and which correlates with the observation that a 3 residue longer loop could be observed in the alignment (Figure 4). This might be able to give additional conformational flexibility to the binding site, allowing the possibility of novel binding modes of the inhibitors that could be stabilized by different hydrogen bonding patterns (Figure 4). For *P. infestans* this idea is supported by the higher number of favorable and structurally different binding modes that the compounds displayed in the top 5 rated positions by the docking procedures. That compared with any of the other models used in this study was almost 3 times bigger (Data not shown).

To date, there is no DHODase crystal structure with a bound ubiquinone available and it is assumed that the natural or artificial acceptors bind to the same place as inhibitors (Hansen *et al*, 2004). We tried to accommodate in the inhibitor binding cavity, 15 compounds of different length that resemble natural DHODase acceptors. As compounds get longer, the higher the number of the rotatable bonds and the harder it is to make more accurate binding prediction. This partially explains why some of the most promising natural acceptors for *P. infestans* DHODase as Dcq-500, Bdl-0, Pqn-501, Umq-1101, Uq1-177 and Uq2-1287 were the shortest of compounds analyzed. In order to guide more accurate binding predictions of the *P. infestans* DHODase we put as a negative control compound fumarate, a short natural electron acceptor of family type 1 DHODases (Andersen *et al*., 1994). The docking results did not detect this compound as a probable *P. infestans* acceptor, which supports our previous findings obtained by the phylogenic analysis for the DHODase as a type 2 enzyme. Our overall data suggest that for *P. infestans* it seems possible that the natural DHODase electron acceptor could be a respiratory quinone. Depicting the fact that not much is known about the Omycetes respiratory chain complexes, it appears by the docking calculations that the nature of this quinone relates more to small physiological electron acceptors of the mitochondrial respiratory chain than to larger ones (Data not shown).
Almost in all cases residue Arg157 was detected making hydrogen bonds, pointing it out as key residue in for the interaction with the acceptor (Figure 2B). Arg 157 was also frequently found interacting in the hydrogen bonding of many of the top-rated inhibitory compounds detected here. These findings agree with those obtained from the rat structure, which pointed to the flexibility and importance of Arg 136 in the binding of the natural acceptor (Hansen *et al*., 2004). In the quest for *P. infestans* specific inhibitors, the interaction with this residue could be used to generate spatial constraints that guide inhibitor search.

3.5 Cloning and expression of the *P. infestans* DHODase

We cloned, sequenced and overexpressed the *P. infestans* DHODase in order to experimentally test the inhibitors compounds predicted by docking. It is quite surprising that no DHODase from any Oomycete had yet been characterized at a molecular level (although, a *P. infestans* mitochondrial bound enzyme has been cloned expressed and purified (Lopez-Calcagno *et al*., 2009)). The putative *P. infestans* DHODase has a longer (17 residues) N-terminal extension than the rat enzyme (Figure 1) and it appears to contain a putative bipartite mitochondrial targeting motif as well as a transmembrane anchor. To accomplish soluble expression of the enzyme, 2 vector constructs were produced to express recombinant proteins, a full-length pET19b-PiDHOD and N-terminally truncated mutant (pET19b-ΔNPiDHOD-PHEW) that lacks the first 54 residues. This strategy has been previously shown to be successful for obtaining soluble expression of DHODases from other organisms, and exerts no effect on the enzyme activity or the inhibitor binding (Ullrich *et al*., 2001, Baldwin *et al*., 2002).
Even though good overexpresion of the of both recombinant *P. infestans* DHODases was achieved with the pET-19b vector in *E. coli* BL21(DE3) cells, the initial purification attempts showed the presence of both recombinant enzymes in the insoluble fraction after sonication in presence of Triton-X 100 and lysozyme (Figure 5A). Using the standard methodology, it was not possible to obtained soluble *P. infestans* DHODase with any of the constructs, not even by changing the time of interaction with the lysis buffer or by using a greater amount of Triton X-100. It is possible that the attachment of even the N-terminus truncated recombinant enzyme to the *E. coli* membrane is a very strong interaction, or that inclusion bodies are produced. However, total solubilization of the full-length enzyme was achieved by the adding denaturation agent SDS at 5% to the mixture. Nevertheless, at this concentration of SDS the protein would need to be refolded to its native structure, and it's possible that the resulting enzyme preparation would be inactive or misfolded. Therefore other methods for obtaining soluble and active protein are currently being tested. Induced *E. coli* cells extracts subject to SDS–PAGE and visualized by Coomassie staining (Figure 5A), showed prominent overexpressed bands with the expected molecular weight range (close to the 49.1kD molecular marker) for the two recombinant *P. infestans*

DHODases. Furthermore, Western blot analysis (Figure 5B) revealed that these induced bands react with the anti-Histag antibodies and their migration properties fully agree with the predicted molecular weight of the full length ~48.54 kD and the truncated ~43.18 kD enzymes. These initial findings provide the basis for the purification of the *P. infestans* recombinant DHODase that could be used in bioassays to search for inhibitors that specifically target the *P. infestans* DHODase (see Discussion). Therefore current efforts continue for the *P. infestans* DHODase as well as for the *P. infestans* host *S. tuberosum*. The inhibition activity assays must be performed with both to further select potential species-selective inhibitors for control strategies.

3.6 Functional analysis of the DHOD sequences

In order to determine if the full length and N-terminally truncated sequences cloned in the expression vector were indeed the *P. infestans* functional DHODases, a complementation assay was performed in an *E. coli* DHODase mutant (*pyrD*(-)). While *pyrD*(-) cells and *pyrD*(-) transformed with parent vector could grow in rich medium, they were unable to grow in minimal media lacking a pyrimidine source. Furthermore, the supplementation of the media with the pyrimidine base uracil was able to restore growth. Variations in the optical density were detected but could likely be explained by traces of intracellular pyrimidines. Both the full-length and the truncated *P. infestans* DHODase vector appeared to complement the pyrimidine deficiency, allowing mutant *pyrD*(–) cells to grow in minimal media (Figure 6). The final optical density values achieved by supplementing with uracil were smaller than those obtained by complementation; this could imply the synthesis of the metabolic intermediates generated by the presence of a DHODase could benefit *E. coli* growth to a greater extent than just supplementing with the pyrimidine base (Yates *et al*., 1957).

These findings support the enzymatic DHODase function predicted for the *P. infestans* annotated DHODase gene. The complementation of *pyrD(–)* cells by both vectors, seem to imply that both recombinant DHODases are functionally active and able to support the pyrimidine auxotrophy. The exact role played by the longer N-terminal extension of the *P. infestans* DHODase remains to be determined, although its association with the recombinant enzyme insolubility in the expression assays could not be ruled out (Neidhardt *et al*., 1999).

4. Concluding remarks and future perspectives

To our knowledge this is the first experimental report of enzymes of *de novo* pyrimidine biosynthesis in *P. infestans* or any other oomycete. According to similar searches, this devastating phytopathogen may be able to meet its metabolic requirement by both salvage and synthesizing pyrimidines *de novo*. The extent to which each pathway is carried out in the different stages of its life cycle must still be determined through biochemical studies. Upon invasion, when the pathogen is undergoing a rapid growth and development, larger amounts of nucleotides are probably required and would be supplied to a greater extent through the *de novo* pathway. We believe that, as is the case for apicomplexan pathogens, the inhibition of the enzymes of this pathway may have a profound effect on the growth and virulence of *P. infestans*.

The bioinformatics tools used to characterize the enzymes that catalyze the six metabolic steps of the pathway, led to the identification of OMPDase and OPRTase as the most promising targets for inhibition as a means to develop novel control strategies. Nevertheless, the careful analysis of not so promising candidates of the pathway such as DHODase suggest that even small structural differences between host and pathogen enzymes could be exploited to develop species-specific inhibitors. Therefore we hope to identify inhibitors for all of the enzymes of the pathway.

In this long-term strategy, the use of predicted enzymes structures and molecular docking procedures may be valuable and inexpensive tools that could lead to discovery of promising inhibitory compounds of the enzymes of the pathway. Using these tools in the *P. infestans* DHODase it was possible to identify three of twenty-nine compounds that exert specific inhibitory effects on the pathogen enzyme and not on the host. With the bigger objective to implement a future virtual screening search of inhibitory

compounds libraries with *P. infestans* enzymes models, we described a set of parameters for DHODase that must be specifically calculated and integrated as constraint settings to improve a counter selective strategy. This will greatly reduce the number of compound in analysis and the need for a high-throughput laboratory screening. With a manageable number of candidate compounds laboratory inhibition tests will be cost-effective. For these purposes the recombinant expression of *P.infestans* membrane bonded DHODase as an active solublilized protein, will allow not only their molecular characterization but also to validate experimentally the candidate compounds found by docking. DHODase from *P. infestans* may be posttranlationally cleavage *in vivo,* so the production of specific antibodies to test this result must be considered.

The key points of the procedure mentioned herein should be carried out with all of the enzymes of the pathway to develop a more robust crop control system based on the synergisms of the multiple metabolic inhibitors of the pyrimidine biosynthesis. This would, in principle, greatly improve its efficiency by decreasing the risks of resistance. Whether a similar inhibitory strategy based on other well-recognized apicomplexan targets would allow efficient crop management is an intriguing question still to be answered.

5. Acknowledgments

We thank la Facultad de Ciencias of the Universidad de los Andes for the funding of this work**.**

6. References

Lamour KH, Win J, Kamoun S; Oomycete genomics: new insights and future directions; FEMS Microbiol Lett. 2007 Sep;274(1):1-8; PMID: 17559387

Attard A, Gourgues M, Galiana E, Panabières F, Ponchet M, Keller H; Strategies of attack and defense in plant-oomycete interactions, accentuated for Phytophthora parasitica Dastur (syn. P. Nicotianae Breda de Haan); J Plant Physiol. 2008 Jan;165(1):83-94; PMID: 17766006

Judelson HS; Genomics of the plant pathogenic oomycete Phytophthora: insights into biology and evolution; Adv Genet. 2007;57:97-141; PMID: 17352903

Fry W; Phytophthora infestans: the plant (and R gene) destroyer; Mol Plant Pathol. 2008 May;9(3):385-402; PMID: 18705878

Nicholls H; Stopping the rot; PLoS Biol. 2004 Jul;2(7):E213; PMID: 15252456

Son SW, Kim HY, Choi GJ, Lim HK, Jang KS, Lee SO, Lee S, Sung ND, Kim JC; Bikaverin and fusaric acid from Fusarium oxysporum show antioomycete activity against Phytophthora infestans; J Appl Microbiol. 2008 Mar;104(3):692-8; PMID: 17927749

Haldar K, Kamoun S, Hiller NL, Bhattacharje S, van Ooij C; Common infection strategies of pathogenic eukaryotes; Nat Rev Microbiol. 2006 Dec;4(12):922-31; PMID: 17088934

Martens C, Vandepoele K, Van de Peer Y; Whole-genome analysis reveals molecular innovations and evolutionary transitions in chromalveolate species; Proc Natl Acad Sci U S A. 2008 Mar 4;105 (9):3427-32; PMID: 18299576

Hyde JE; Targeting purine and pyrimidine metabolism in human apicomplexan parasites; Curr Drug Targets. 2007 Jan;8(1):31-47; PMID: 17266529

Schroder M, Giermann N, Zrenner R; Functional Analysis of the Pyrimidine de Novo Synthesis Pathway in Solanaceous Species; Plant Physiology. Aug 2005; 138: 1926–1938; PMID: 16024685

Evans DR, Guy HI; Mammalian pyrimidine biosynthesis: fresh insights into an ancient pathway; J Biol Chem. 2004 Aug 6;279(32):33035-8; PMID: 15096496

Löffler M, Fairbanks LD, Zameitat E, Marinaki AM, Simmonds HA; Pyrimidine pathways in health and disease; Trends Mol Med. 2005 Sep;11(9):430-7; PMID: 16098809

Clark MC, Melanson DL, Page OT; Purine metabolism and differential inhibition of spore germination in Phytophthora infestans; Can J Microbiol. 1978 Sep; 24(9):1032-8; PMID: 709431

Christopherson RI, Lyons SD, Wilson PK; Inhibitors of de novo nucleotide biosynthesis as drugs; Acc Chem Res. 2002 Nov;35(11):961-71; PMID: 12437321

Fox BA, Bzik DJ.; De novo pyrimidine biosynthesis is required for virulence of Toxoplasma gondii; Nature. 2002 Feb 21; 415(6874):926-9; PMID: 11859373

Kovarik JM, Burtin P; Immunosuppressants in advanced clinical development for organ transplantation and selected autoimmune diseases; Expert Opin Emerg Drugs. 2003 May; 8(1):47-62; PMID: 14610911

Herrmann ML, Schleyerbach R, Kirschbaum BJ; Leflunomide: an immunomodulatory drug for the treatment of rheumatoid arthritis and other autoimmune diseases; Immunopharmacology. 2000 May;47(2-3):273-89; PMID: 10878294

Rückemann K, Fairbanks LD, Carrey EA, Hawrylowicz CM, Richards DF, Kirschbaum B, Simmonds HA; Leflunomide inhibits pyrimidine de novo synthesis in mitogen-stimulated T-lymphocytes from healthy humans; J Biol Chem. 1998 Aug 21;273(34):21682-91; PMID: 9705303

Deng X, Gujjar R, El Mazouni F, Kaminsky W, Malmquist NA, Goldsmith EJ, Rathod PK, Phillips MA; Structural plasticity of malaria dihydroorotate dehydrogenase allows selective binding of diverse chemical scaffolds; J Biol Chem. 2009 Sep 25;284(39):26999-7009; PMID: 19640844

Geigenberger P, Regierer B, Nunes-Nesi A, Leisse A, Urbanczyk-Wochniak E, Springer F, van Dongen JT, Kossmann J, Fernie AR; Inhibition of de novo pyrimidine synthesis in growing potato tubers leads to a compensatory stimulation of the pyrimidine salvage pathway and a subsequent increase in biosynthetic performance; Plant Cell. 2005 Jul; 17(7):2077-88. Epub 2005 Jun 10; PMID: 15951490

Knecht W, Henseling J, Löffler M; Kinetics of inhibition of human and rat dihydroorotate dehydrogenase by atovaquone, lawsone derivatives, brequinar sodium and polyporic acid; Chem Biol Interact. 2000 Jan 3;124(1):61-76; PMID: 10658902

Rarey M, Kramer B, Lengauer T; Time-efficient docking of flexible ligands into active sites of proteins; Proc Int Conf Intell Syst Mol Biol. 1995; 3:300-8; PMID: 7584452

Ananthula RS, Ravikumar M, Pramod AB, Madala KK, Mahmood SK; Strategies for generating less toxic P-selectin inhibitors: pharmacophore modeling, virtual screening and counter pharmacophore screening to remove toxic hits; J Mol Graph Model. 2008 Nov;27(4):546-57; PMID: 18993099.

Pospisil P, Kuoni T, Scapozza L, Folkers G; Methodology and problems of protein-ligand docking: case study of dihydroorotate dehydrogenase, thymidine kinase, and phosphodiesterase 4; J Recept Signal Transduct Res. 2002 Feb-Nov;22(1-4):141-54; PMID: 12503612

Vargas AM, Quesada Ocampo LM, Céspedes MC, Carreño N, González A, Rojas A, Zuluaga AP, Myers K, Fry WE, Jiménez P, Bernal AJ, Restrepo S; Characterization of Phytophthora infestans populations in Colombia: first report of the A2 mating type; Phytopathology. 2009 Jan; 99(1):82-8; PMID: 19055438

Goodwin SB, Smart CD, Sandrock RW, Deahl KL, Punja ZK, Fry WE; Genetic Change Within Populations of Phytophthora infestans in the United States and Canada During 1994 to 1996: Role of Migration and Recombination; Phytopathology. 1998 Sep;88(9):939-49; PMID: 18944872

Goodwin SB, Drenth A, Fry WE; Cloning and genetic analyses of two highly polymorphic, moderately repetitive nuclear DNAs from Phytophthora infestans; Curr Genet. 1992 Aug;22(2):107-15; PMID: 1358466

van West P, de Jong AJ, Judelson HS, Emons AM, Govers F; The ipiO gene of Phytophthora infestans is highly expressed in invading hyphae during infection; Fungal Genet Biol. 1998 Mar;23(2):126-38; PMID: 9578626

Baldwin J, Farajallah AM, Malmquist NA, Rathod PK, Phillips MA; Malarial dihydroorotate dehydrogenase. Substrate and inhibitor specificity; J Biol Chem. 2002 Nov 1;277(44):41827-34; PMID: 12189151

Ullrich A, Knecht W, Fries M, Löffler M; Recombinant expression of N-terminal truncated mutants of the membrane bound mouse, rat and human flavoenzyme dihydroorotate dehydrogenase. A versatile tool to rate inhibitor effects?; Eur J Biochem. 2001 Mar;268(6):1861-8; PMID: 11248707

Laemmli UK; Cleavage of structural proteins during the assembly of the head of bacteriophage T4; Nature. 1970 Aug 15;227(5259):680-5; PMID: 5432063

Sierra Pagan ML, Zimmermann BH; Cloning and expression of the dihydroorotate dehydrogenase from Toxoplasma gondii; Biochim Biophys Acta. 2003 Mar 20;1637(2):178-81; PMID: 12633907

Zimmermann BH, Evans DR; Cloning, overexpression, and characterization of the functional dihydroorotase domain of the mammalian multifunctional protein CAD; Biochemistry. 1993 Feb 16;32(6):1519-27; PMID: 8094297

Nara T, Hshimoto T, Aoki T; Evolutionary implications of the mosaic pyrimidine-biosynthetic pathway in eukaryotes; Gene. 2000 Oct 31;257(2):209-22; PMID: 11080587

Edgar RC; MUSCLE: a multiple sequence alignment method with reduced time and space complexity; BMC Bioinformatics. 2004 Aug 19;5:113; PMID: 15318951

Guindon S, Gascuel O; A simple, fast, and accurate algorithm to estimate large phylogenies by maximum likelihood; Syst Biol. 2003 Oct;52(5):696-704; PMID: 14530136

Schwede T, Kopp J, Guex N, Peitsch MC; SWISS-MODEL: An automated protein homology-modeling server; Nucleic Acids Res. 2003 Jul 1;31(13):3381-5; PMID: 12824332

Hurt, D.E., Sutton, A.E., Clardy, J; Brequinar derivatives and species-specific drug design for dihydroorotate dehydrogenase; Bioorg Med Chem Lett. 2006 Mar 15;16(6):1610-5; PMID: 16406782

Thompson JD, Higgins DG, Gibson TJ; CLUSTAL W: improving the sensitivity of progressive multiple sequence alignment through sequence weighting, position-specific gap penalties and weight matrix choice; Nucleic Acids Res. 1994 Nov 11;22(22):4673-80. PMID: 7984417

Kaplan W, Littlejohn TG; Swiss-PDB Viewer (Deep View); Brief Bioinform. 2001 May;2(2):195-7;PMID: 11465736

Guex N, Peitsch MC; SWISS-MODEL and the Swiss-PdbViewer: an environment for comparative protein modeling; Electrophoresis. 1997 Dec;18(15):2714-23; PMID: 9504803

Thomsen R, Christensen MH; MolDock: a new technique for high-accuracy molecular docking; J Med Chem. 2006 Jun 1;49(11):3315-21; PMID: 16722650

Sivaprakasam P, Tosso PN, Doerksen RJ; Structure-activity relationship and comparative docking studies for cycloguanil analogs as PfDHFR-TS inhibitors; J Chem Inf Model. 2009 Jul;49(7):1787-96; PMID: 19588935

Khan MT, Fuskevåg OM, Sylte I; Discovery of potent thermolysin inhibitors using structure based virtual screening and binding assays; J Med Chem. 2009 Jan 8;52(1):48-61; PMID: 19072688

Cassidy CE, Setzer WN; Cancer-relevant biochemical targets of cytotoxic Lonchocarpus flavonoids: A molecular docking analysis; J Mol Model. 2009 Jul 15; PMID: 19603203

Morris PF, Schlosser LR, Onasch KD, Wittenschlaeger T, Austin R, Provart N; Multiple horizontal gene transfer events and domain fusions have created novel regulatory and metabolic networks in the oomycete genome; PLoS One. 2009 Jul 2;4(7):e6133; PMID: 19582169

Makiuchi T, Nara T, Annoura T, Hashimoto T, Aoki T; Occurrence of multiple, independent gene fusion events for the fifth and sixth enzymes of pyrimidine biosynthesis in different eukaryotic groups; Gene. 2007 Jun 1;394(1-2):78-86; PMID: 17383832

Makiuchi T, Annoura T, Hashimoto T, Murata E, Aoki T, Nara T; Evolutionary analysis of synteny and gene fusion for pyrimidine biosynthetic enzymes in Euglenozoa: an extraordinary gap between kinetoplastids and diplonemids; Protist. 2008 Jul;159(3):459-70. Epub 2008 Apr 3; PMID: 18394957

Nørager S, Jensen KF, Björnberg O, Larsen S; E. coli dihydroorotate dehydrogenase reveals structural and functional distinctions between different classes of dihydroorotate dehydrogenases; Structure. 2002 Sep;10(9):1211-23; PMID: 12220493

Sørensen G, Dandanell G; A new type of dihydroorotate dehydrogenase, type 1S, from the thermoacidophilic archaeon Sulfolobus solfataricus; Extremophiles. 2002 Jun;6(3):245-51. Epub 2002 Mar 15; PMID: 12072960

Altschul SF, Madden TL, Schäffer AA, Zhang J, Zhang Z, Miller W, Lipman DJ; Gapped BLAST and PSI-BLAST: a new generation of protein database search programs; Nucleic Acids Res. 1997 Sep 1;25(17):3389-402; PMID: 9254694

Hansen M, Le Nours J, Johansson E, Antal T, Ullrich A, Löffler M, Larsen S; Inhibitor binding in a class 2 dihydroorotate dehydrogenase causes variations in the membrane-associated N-terminal domain; Protein Sci. 2004 Apr;13(4):1031-42; PMID: 15044733

Löffler M, Knecht W, Rawls J, Ullrich A, Dietz C; Drosophila melanogaster dihydroorotate dehydrogenase: the N-terminus is important for biological function in vivo but not for catalytic properties in vitro; Insect Biochem Mol Biol. 2002 Sep;32(9):1159-69; PMID: 12213251

Knecht W, Löffler M; Species-related inhibition of human and rat dihydroorotate dehydrogenase by immunosuppressive isoxazol and cinchoninic acid derivatives; Biochem Pharmacol. 1998 Nov 1;56(9):1259-64; PMID: 9802339

Rawls J, Knecht W, Diekert K, Lill R, Löffler M; Requirements for the mitochondrial import and localization of dihydroorotate dehydrogenase; Eur J Biochem. 2000 Apr;267(7):2079-87; PMID: 10727948

Emanuelsson O, Nielsen H, Brunak S, von Heijne G; Predicting subcellular localization of proteins based on their N-terminal amino acid sequence; J Mol Biol. 2000 Jul 21;300(4):1005-16; PMID: 10891285

Claros MG, Vincens P; Computational method to predict mitochondrially imported proteins and their targeting sequences; Eur J Biochem. 1996 Nov 1;241(3):779-86; PMID: 8944766

Jones ME; Pyrimidine nucleotide biosynthesis in animals: genes, enzymes, and regulation of UMP biosynthesis; Annu Rev Biochem. 1980;49:253-79; PMID: 6105839

Björnberg O, Rowland P, Larsen S, Jensen KF. Biochemistry; Active site of dihydroorotate dehydrogenase A from Lactococcus lactis investigated by chemical modification and mutagenesis; 1997 Dec 23;36(51):16197-205; PMID: 9405053

Yates RA, Pardee AB; Control by uracil of formation of enzymes required for orotate synthesis; J Biol Chem. 1957 Aug;227(2):677-92; PMID: 13462990

Neidhardt EA, Punreddy SR, McLean JE, Hedstrom L, Grossman TH; Expression and characterization of E. coli-produced soluble, functional human dihydroorotate dehydrogenase: a potential target for immunosuppression; J Mol Microbiol Biotechnol. 1999 Aug;1(1):183-8; PMID: 10941801

Singh S, Malik BK, Sharma DK; Molecular modeling and docking analysis of Entamoeba histolytica glyceraldehyde-3 phosphate dehydrogenase, a potential target enzyme for anti-protozoal drug development; Chem Biol Drug Des. 2008 Jun; 71(6): 554-62; PMID: 18489439

Baumgartner R, Walloschek M, Kralik M, Gotschlich A, Tasler S, Mies J, Leban J; Dual binding mode of a novel series of DHODH inhibitors; J Med Chem. 2006 Feb 23;49(4):1239-47; PMID: 16480261

Arnold K., Bordoli L., Kopp J., and Schwede T; The SWISS-MODEL Workspace: A web-based environment for protein structure homology modeling; Bioinformatics. 2006 Jan 15;22(2):195-201; PMID: 16301204

Katahira R, Ashihara H; Profiles of pyrimidine biosynthesis, salvage and degradation in disks of potato (Solanum tuberosum L.) tubers; Planta. 2002 Sep;215(5):821-8; PMID: 12244448

Ananthula RS, Ravikumar M, Pramod AB, Madala KK, Mahmood SK; Strategies for generating less toxic P-selectin inhibitors: pharmacophore modeling, virtual screening and counter pharmacophore screening to remove toxic hits; J Mol Graph Model. 2008 Nov;27(4):546-57; PMID: 18993099

Baldwin J, Michnoff CH, Malmquist NA, White J, Roth MG, Rathod PK, Phillips MA; High-throughput screening for potent and selective inhibitors of Plasmodium falciparum dihydroorotate dehydrogenase; J Biol Chem. 2005 Jun 10;280(23):21847-53; PMID: 15795226

Phillips MA, Gujjar R, Malmquist NA, White J, El Mazouni F, Baldwin J, Rathod PK; Triazolopyrimidine-based dihydroorotate dehydrogenase inhibitors with potent and selective activity against the malaria parasite Plasmodium falciparum; J Med Chem. 2008 Jun 26;51(12):3649-53; PMID: 18522386

Andersen PS, Jansen PJ, Hammer K; Two different dihydroorotate dehydrogenases in Lactococcus lactis; J Bacteriol. 1994 Jul;176(13):3975-82; PMID:8021180

López-Calcagno PE, Moreno J, Cedeño L, Labrador L, Concepción JL, Avilán L; Cloning, expression and biochemical characterization of mitochondrial andcytosolic malate dehydrogenase from Phytophthora infestans; Mycol Res. 2009, Jun-Jul;113(Pt 6-7):771-81; PMID: 19249364

Walse B, Dufe VT, Svensson B, Fritzson I, Dahlberg L, Khairoullina A, Wellmar U, Al-Karadaghi S; The structures of human dihydroorotate dehydrogenase with and without inhibitor reveal conformational flexibility in the inhibitor and substrate binding sites; Biochemistry. 2008 Aug 26;47(34):8929-36; PMID: 18672895

Stroganov OV, Novikov FN, Stroylov VS, Kulkov V, Chilov GG; Lead finder: an approach to improve accuracy of protein-ligand docking, binding energy estimation, and virtual screening; J Chem Inf Model. 2008 Dec;48(12):2371-85.PMID: 19007114

Spyrakis F, Amadasi A, Fornabaio M, Abraham DJ, Mozzarelli A, Kellogg GE, Cozzini P; The consequences of scoring docked ligand conformations using free energy correlations; Eur J Med Chem. 2007 Jul;42(7):921-33; PMID: 17346861

7. Figures and tables

Table 1. Summary and architecture of the *P. infestans* pyrimidine biosynthetic genes.

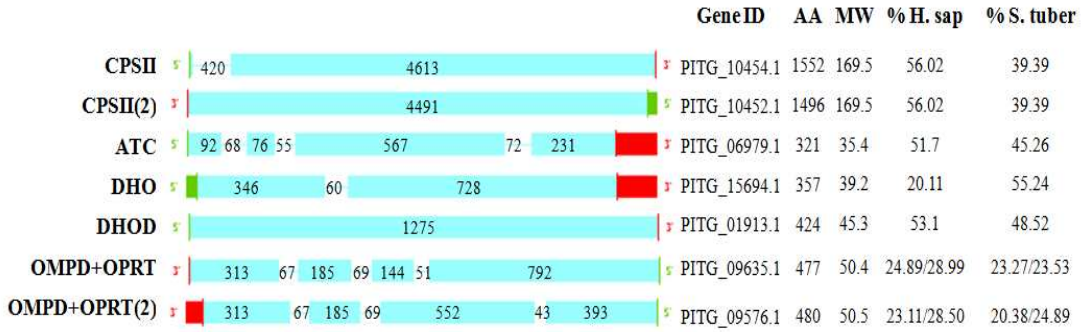

Table 1. Graphical representation of the *P. infestans* putative nucleotide sequences that code for the enzymes of the *de novo* pyrimidine biosynthetic pathway. Gene information was retrieved from the genome project (http://www.broadinstitute.org). CPSII: Carbamoyl phosphate synthase II, ATC: aspartate transcarbamoylase, DHO: dihydroorotase, DHOD: dihydroorotate dehydrogenase, OPRT: orotate phosphoribosyl transferase and OMPD: orotidine 5′-monophosphate decarboxylase. The relative sizes of the nucleotide sequences in base pairs are shown in black; introns are colored in aquamarine while exons are in white. The length (AA), predicted weight (MW) in kDa, percent of identity with *S. tuberosum* putative sequences (%H.sap), percent identity with *H. sapiens* sequences (%S.tuber) and gene ID are for the amino acid sequences.

Table 2. Scores derived from the MVD docking.

	PDB	Compound	Formula	*P. infestans*		*S. tuberosum*		*P. falciparum*		*H. sapiens*	
Type of compound	Type of score			Moldock	Rerank	Moldock	Rerank	Moldock	Rerank	Moldock	Rerank
A77-1726	1TV5	a26-1001	$C_{12}H_{11}F_3N_2O_2$	-113,612	-96,444	-107,674	-92,283	-122,969	-104,83	-110,776	-96,735
Triazolopyrimidine-based	3I6R	**j5z-1001**	$C_{13}H_{10}F_3N_5$	**-130,717**	**-102,33**	**-120,717**	**-95,789**	-141,189	-113,54	-131,7	-106,31
Triazolopyrimidine-based	3I65	**jz8-1001**	$C_{16}H_{15}N_5$	**-139,811**	**-114,13**	**-124,361**	**-99,54**	-144,867	-118,66	-128,567	-97,625
Leflunomide derivative	3FJ6	cih-399	$C_{17}H_{12}Cl_2N_2O_2$	-121,838	-102,74	-133,464	-111,04	-139,294	-107,03	-123,076	-105,07
Leflunomide derivative	3F1Q	bce-397	$C_{17}H_{14}N_2O_2$	-119,147	-100,92	-123,887	-104,91	-129,473	-102,87	-117,9	-101,96
Leflunomide derivative	3G0U	mdy-2	$C_{18}H_{15}ClN_2O_3$	-130,261	-98,769	-135,401	-112,64	-140,164	-94,876	-126,318	-91,177
Brequinar Analog	2FPV	ilc-405	$C_{19}H_{14}FNO_4S$	-160,025	-127,66	-146,92	-111,15	-144,287	-18,585	-171,087	-137,03
Brequinar Analog	2FPY	ilf-407	$C_{19}H_{10}F_5NO_4S$	-157,51	-126,78	-157,77	-130,63	-152,636	-4,582	-162,164	-126,2
Leflunomide derivative	3FJL	cjh-399	$C_{19}H_{18}N_2O_3$	-130,969	-108,59	-134,427	-108,57	-143,201	-102,34	-136,457	-115,68
Leflunomide derivative	3G0X	md7-2	$C_{19}H_{16}N_2O_2$	-128,739	-108,76	-141,752	-117,44	-134,825	-102,99	-134,042	-106,93
Brequinar Analog	2FQI	ilh-600	$C_{20}H_{10}F_7NO_4$	-168,22	-135,67	-170,294	-133,13	-141,89	-13,354	-180,123	-147,47
Brequinar Analog	2FPT	ilb-405	$C_{20}H_{14}F_5NO_4$	-167,459	-134,91	-168,186	-133,26	-144,018	-45,914	-182,107	-143,43
Brequinar Analog	2B0M	201-401	$C_{20}H_{15}NO_3$	-140,349	-115,65	-143,386	-118,42	-126,874	-21,751	-154,553	-130,83
Triazolopyrimidine-based	3I68	jz4-1001	$C_{20}H_{15}N_5$	-145,114	-69,288	-135,235	-106,67	-143,873	-100,08	-142,578	-77,499
Brequinar Analog	2BXV	3ft-1401	$C_{20}H_{15}F_4NO_4$	-160,344	-106,55	-159,172	-123,72	-141,161	-51,167	-164,1	-134,4
Brequinar Analog	2PRL	2rc-400	$C_{20}H_{17}NO_4$	-136,599	-109,12	-141,908	-118,17	-143,414	-75,661	-147,574	-120,08
Atovaquone	1UUM	**afi-400**	$C_{22}H_{19}ClO_3$	**-135,418**	**-117,73**	**-120,578**	**-98,389**	-122,471	-74,537	-146,603	-125,71
Brequinar	1UUO	brf-1397	$C_{23}H_{15}F_2NO_2$	-145,496	-114,53	-146,459	-110,9	-111,593	27,405	-181,815	-148,89
Leflunomide derivative	2PRH	238-400	$C_{23}H_{15}ClFNO_2$	-148,418	-115,36	-150,907	-120,28	-118,217	35,945	-177,543	-147,24
Brequinar Analog	1D3G	bre397	$C_{23}H_{16}FNO_2$	-119,914	-90,267	-138,817	-107,21	-115,254	8,14	-165,602	-136,78

Table 2. Part of the Molegro virtual docker results obtained for 20 compounds in DHODase structures, only the best position is show. Moldock and Rerank energy scores (arbitrary units). Selected compound scores predicted as the top rated inhibitors are in grey. In bold, counter-selected compounds that exert no effect over the *S. tuberosum* DHODase.

Figure 1. *P. infestans* DHOD sequence alignment

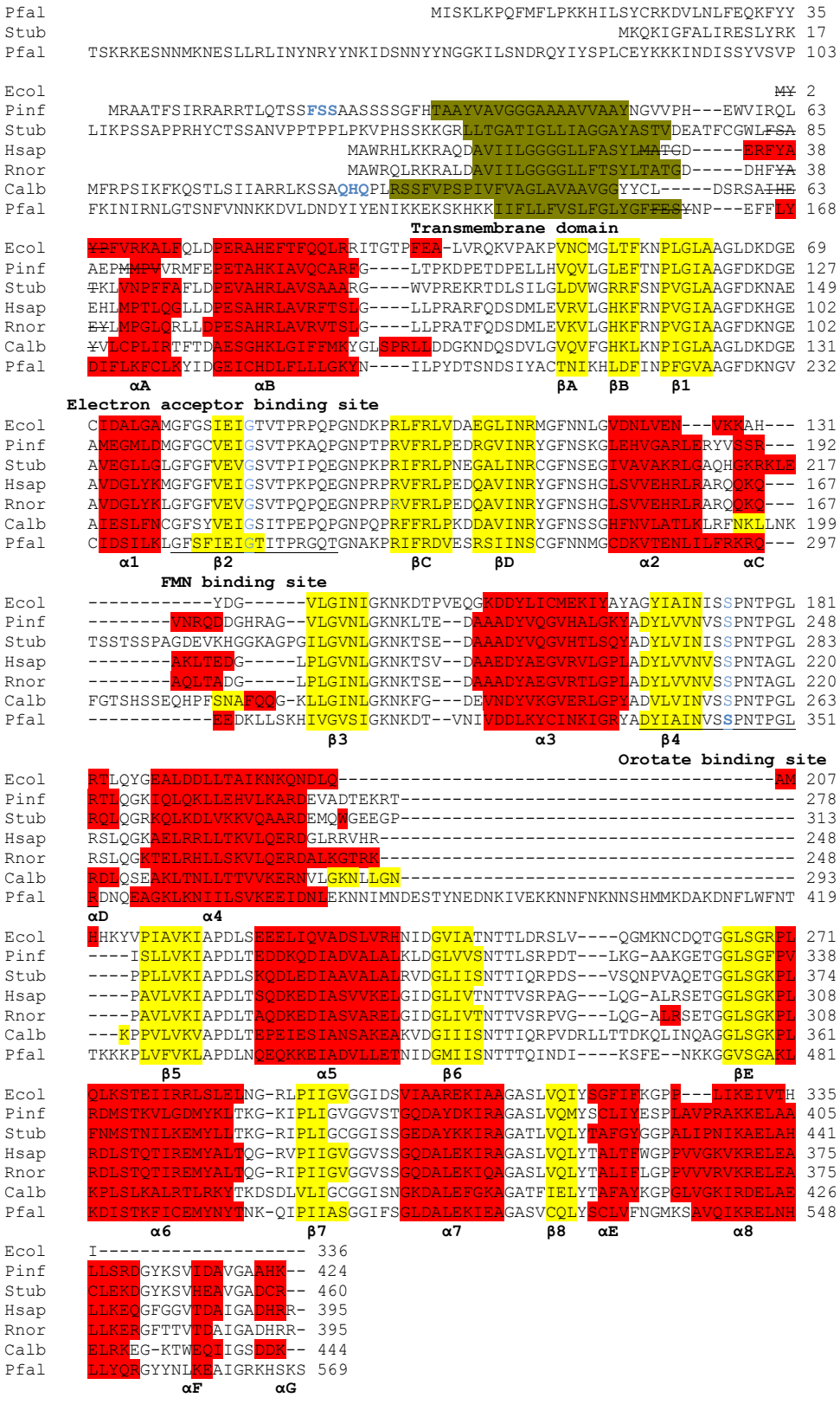

Figure 1. Alignment of the *P. infestans* DHODase predicted amino acid sequence with other family 2 DHODases. Secondary structural representation of the DHODases motives from de PDB-viewer; alpha helices show in red and beta sheets in yellow. The beginning of the 3D structures shown as strikeout. Alpha-helixes in the central barrel are named α_1-α_8, and β-sheets in the barrel are named β_1-β_8. α-Helixes and β-sheets outside the barrel are named α_A-α_G and β_A-β_E. The N-terminal trasmembrane domains predicted by HMMTOP are shown in green. MitoprotII predicted cleavage sites in blue. FMN and orotate binding sites, are underlined.

Figure 2. Structural model of the *P. infesatans* DHODase

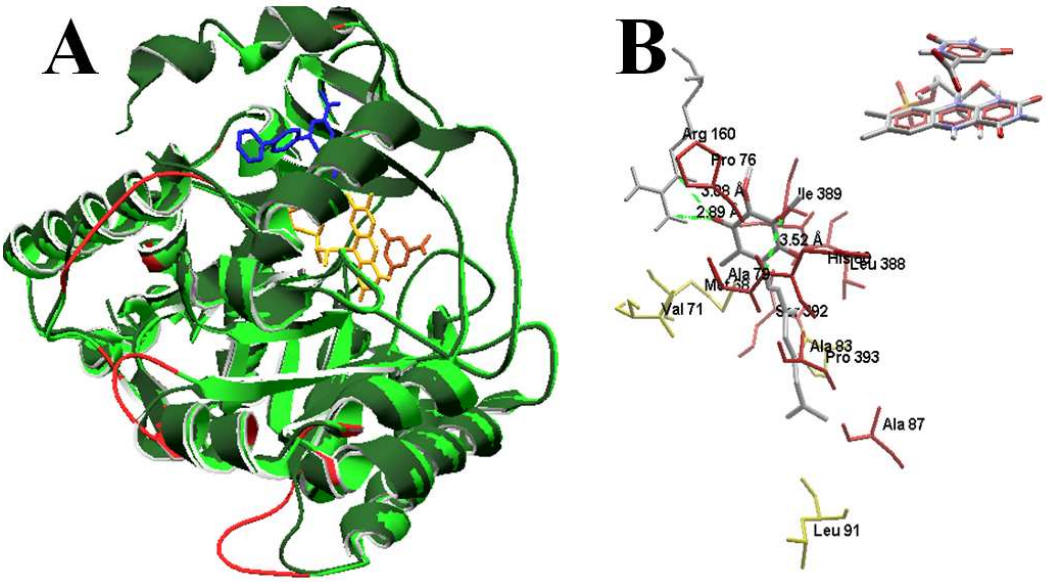

Figure 2. **Panel A.** Ribbon diagram showing the overall structure of the DHODase used as template (Dark green, PDB:2B0M) and the *Phytophthora* DHODase predicted structure (Ligth green). Unconcordat regions colored by B-factor shown in red, human inhibitor (201-401) in blue, cofactor in yellow (FMN) and product in brown (orotate). **Panel B.** *P. infestans* residues at 6Å from ubiquinone 2 (center), hidrogen bonds show in green. Upper right FMN and Orotate. Residues colored by type and depth. These figures were produced by Swiss PDB-Vierwer (A) and by the Molegro virtual Docker (B)

Figure 3. DHOD phylogeny tree.

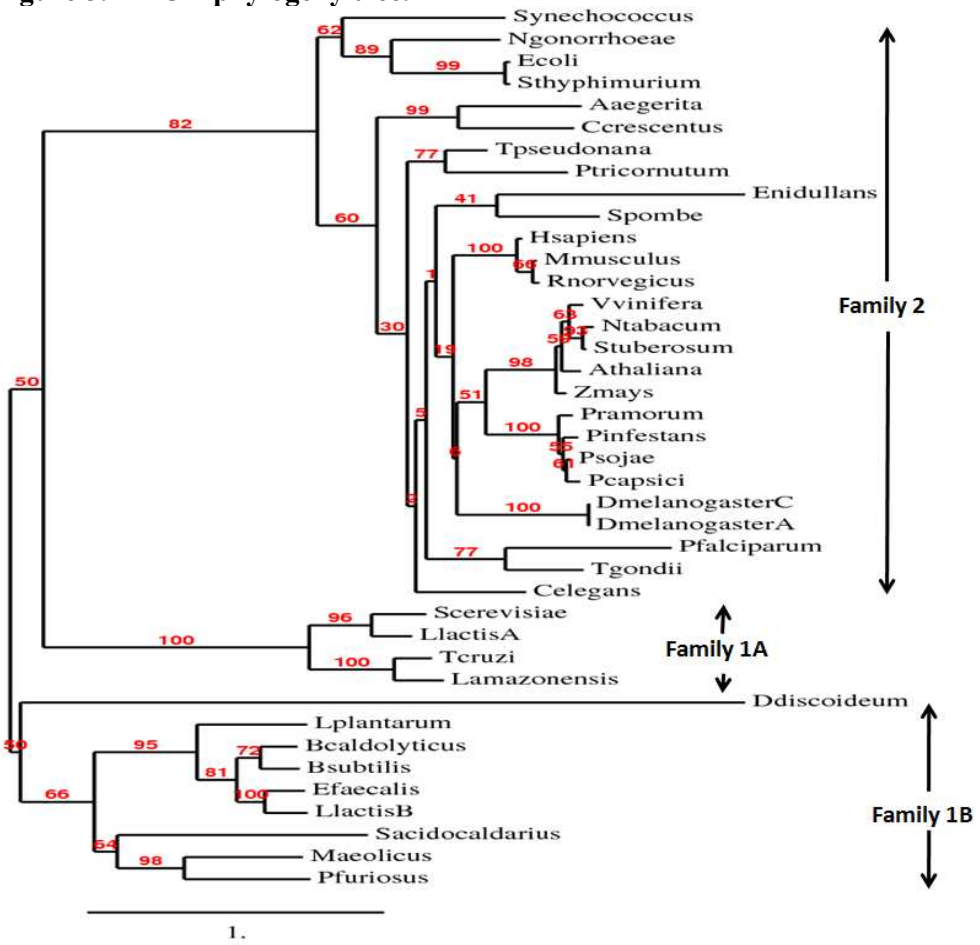

Figure. 3. PhyML tree of the dihydroorotate dehydrogenase (DHODase) sequences, constructed using the Maximun likehood (ML) method which relates protein sequences by the substitution model LG+I+G. The length of the branch is proportional to the estimated number of substitutions.

Figure 4. Docking conformations of compound J5Z-1001

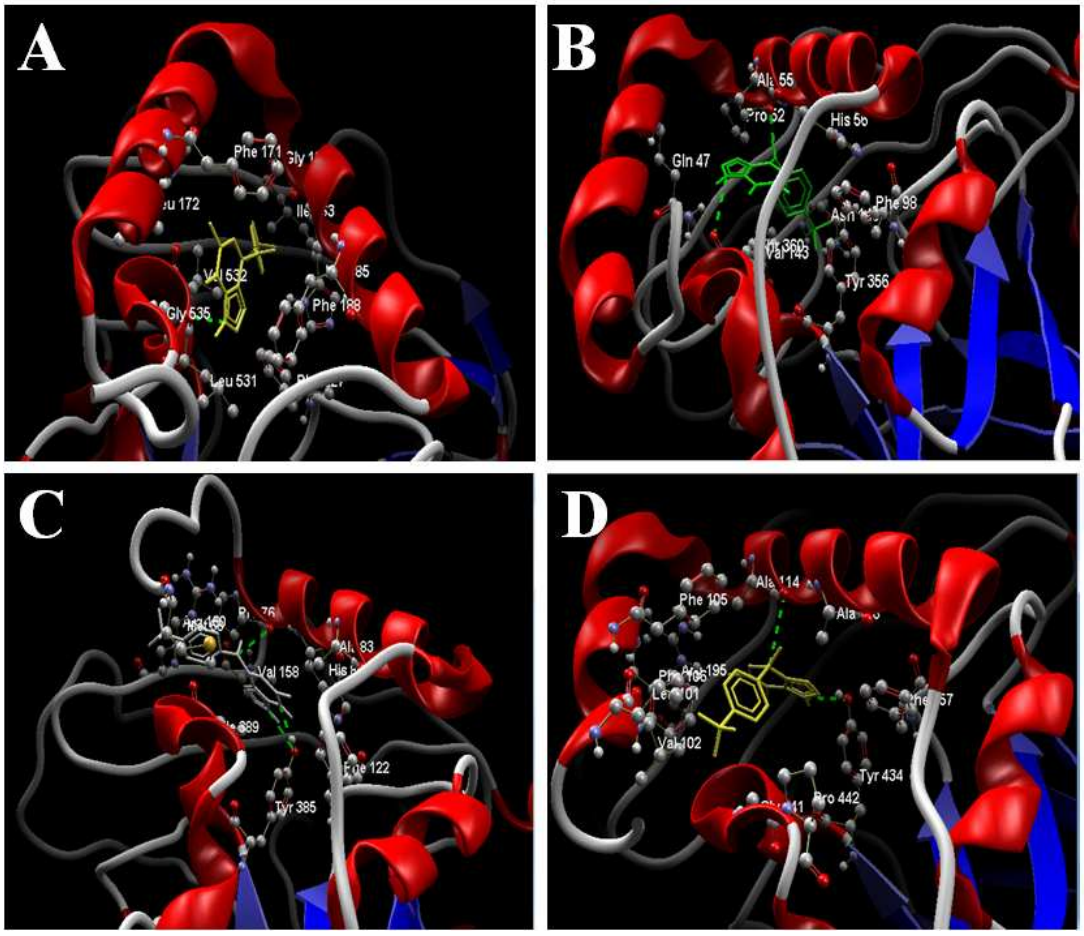

Figure 4. Docked conformation of the most promising compound in the active site of the DHODase structures. Alpha helices displayed in red and beta-sheets in blue. Residues at 7Å from the compound are displayed. Broken green lines represent hydrogen bonds. **Panel A**: *P. falciparum* **Panel B**: *H. sapiens.* **Panel C**: *P. infestans* **Panel D**: *S. tuberosum*.

Figure 5. SDS-PAGE and Western blot of the recombinant *P. infestans* DHODase.

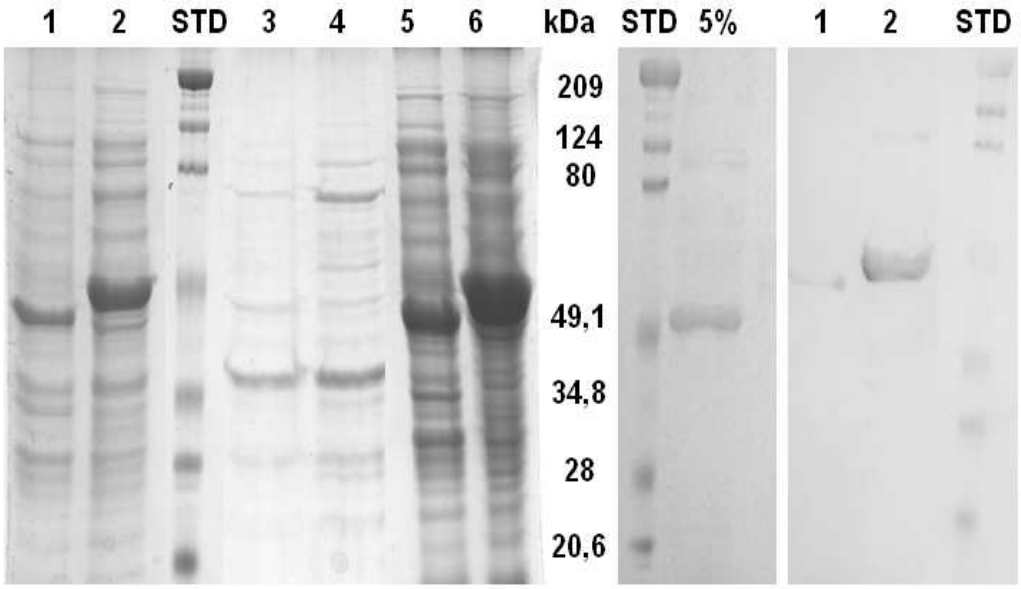

Figure 5. Recombinant *P. infestans* full-length (PiDHODase) and N-terminally truncated (ΔNPiDHODase) dihydroorotate dehydrogenase (DHODase). The N-terminus truncated DHODase in *lanes* 1,3,5 while the full length in *lanes* 2,4 and 6. **Left and central panel.** The ΔNPiDHOD-PHEW and PiDHOD recombinant proteins were subjected to SDS–PAGE and visualized by staining with Coomassie Blue dye. **Right panel.** Western Blot to detect the N-terminally truncated and the full-length recombinant DHODases. ***Lanes 1,2:*** *E. coli* extracts of IPTG induced sonicated cells in presence of 2 % Triton X-100 before centrifugation. ***Lanes 3,4:*** Supernatant of *E. coli* induced cells after centrifugation. ***Lanes 5,6:*** Pellet of *E. coli* induced PiDHODase cells after centrifugation. **Lane 5%:** Supernatant obtained after incubating the full-length recombinant protein pellet in 5% SDS for 30 minutes. **STD**: molecular mass marker.

Figure 6. DHODase Complemetation assay

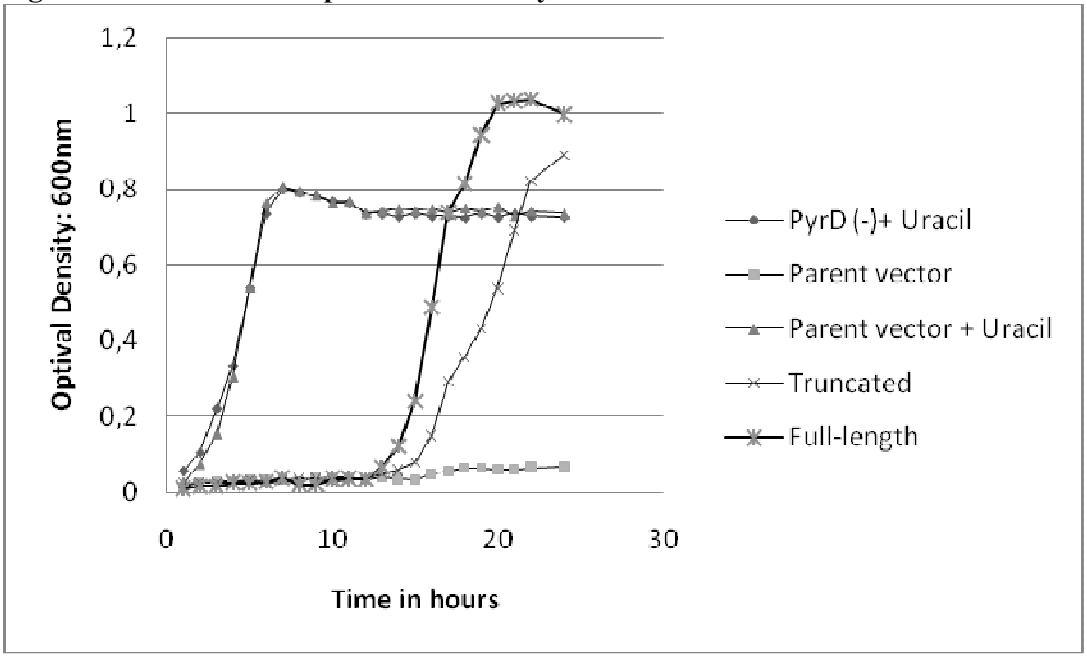

Figure 6. Both recombinant *P. infestans* DHODases complement a DHODase-deficient *E. coli* strain (ATCC12632). *E. coli* cells (*PyrD*(-)) were transformed with parent vector and with the constructs expressing the full-length and truncated *P. infestans* DHODase. Cells were grown in minimal media lacking uracil and growth monitored by optical density measurements al 600nm. *PyrD + Uracil*: *E. coli* cell growth in presence of 12ug/ml uracil; *Parent vector*: Topo-TA; *Parent vector + Uracil*: transformed cell with TOPO vector growth in presence of 12ug/ml uracil; *Truncated*: cells transformed with the *P. infestans* truncated DHODase; *Full-length*: cells transformed with the *P. infestans* full length DHODase.